Article ID: 1006-8775(2020) 04-0441-12

# Statistical and Comparative Analysis of Tropical Cyclone Activity over the Arabian Sea and Bay of Bengal (1977−2018)

FAN Xiao-ting (樊晓婷)[1], LI Ying (李 英)[1], LYU Ai-min (吕爱民)[2], LIU Long-sheng (柳龙生)[2]
(1. State Key Laboratory of Severe Weather, Chinese Academy of Meteorological Sciences, Beijing 100081 China;
2. National Meteorological Center, Beijing 100081 China)

**Abstract:** A statistical comparative analysis of tropical cyclone activity over the Arabian Sea (AS) and Bay of Bengal (BoB) has been conducted using best-track data and wind radii information from 1977 to 2018 issued by the Joint Typhoon Warning Center. Results show that the annual variation in the frequency and duration of tropical cyclones has significantly increased over time over the AS and insignificantly decreased over the BoB. The monthly frequency of tropical cyclones over the AS and the BoB shows a notable bimodal character, with peaks occurring in May and October-November, respectively. The maximum frequency of tropical cyclones occurs in the second peak as a result of the higher moisture content at mid-levels in the autumn. However, the largest proportion of strong cyclones (H1-H5 grades) occurs in the first peak as a result of the higher sea surface temperatures in early summer. Tropical cyclones over the AS break out later during the first peak and activity ends earlier during the second peak, in contrast with those over the BoB. This is related to the onset and drawback times of the southwest monsoon in the two basins. Tropical cyclones over the AS are mainly generated in the eastern basin, whereas in the BoB the genesis locations are meridionally (zonally) distributed in May-June (October-November) as a result of the seasonal movement of the low-level positive vorticity belt. The Arabian Sea is dominated by tropical cyclones that track west and northwest, accounting for about 74.6% of all the tropical cyclones there, whereas the tropical cyclones with a NE track account for only 25.4%. The proportions of the three types of tracks are similar in the BoB, with each accounting for about 33% of the tropical cyclones. The mean intensity and size of tropical cyclones over the AS are stronger and larger, respectively, than those over the BoB and the size of tropical cyclones over the North Indian Ocean in early summer is larger than that in the autumn. The asymmetrical structure of tropical cyclones over the North Indian Ocean is affected by topography and the longest radius of the 34 kt surface wind often lies in the eastern quadrant of the tropical cyclone circulation in both sea areas.

**Key words:** Arabian Sea; Bay of Bengal; tropical cyclones; statistical characteristics
**CLC number:** P444 **Document code:** A
https://doi.org/10.46267/j.1006-8775.2020.038

## 1 INTRODUCTION

Tropical cyclones are severe weather systems that mainly occur in the western and eastern North Pacific Ocean, the North Atlantic Ocean, the North Indian Ocean (NIO), the South Indian Ocean and the South Pacific Ocean (Riehl [1]). Among them, the NIO, including the Arabian Sea and the Bay of Bengal (BoB), contributes only 13% to the total global annual storms (Gary [2]). However, storm disasters in this region are particularly serious as a result of the trumpet terrain of the two seas and the dense coastal population (Chutia et al. [3]). Historical cyclone records show that seven of the ten most deadly cyclones occurred in the BoB (Li et al. [4]). Tropical cyclones over the BoB interact with other systems, such as the south branch trough and the subtropical jet stream, and, as a result, have a great impact on precipitation in southwestern (SW) China, leading to torrential rain, snowstorms, floods and debris flows.

From the climatological point of view, tropical cyclones over the NIO have features that are different from cyclones in other basins (Pattanaik [5]; Camargo et al. [6]). The annual cycle of tropical cyclones in the NIO shows a prominent bimodal feature, with peaks occurring in the monsoon transition periods of April-May and October-November, whereas a single peak is dominant in other basins. This is because the monsoon trough is located far inland during the summer in the region of the NIO and the prevailing southwesterly winds and upper-level easterly winds create strong vertical shear that suppresses the formation of tropical cyclones (Jadhav and Munot [7]). By contrast, the barotropic instability caused by horizontal wind shear can trigger storm formation during the northward advancement of the monsoon trough in the spring or the southward withdrawal of the monsoon trough in the autumn, with the energy for storm development obtained from the basic zonal flow (Krishnamurti et al. [8]; Mao and Wu [9]). November 1−10 is considered to be the most

**Received** 2020-05-07 **Revised** 2020-08-15 **Accepted** 2020-11-15
**Funding:** National Natural Science Foundation of China (41930972, 51778617); S&T Development Fund of CAMS (2020KJ019)
**Biography:** FAN Xiao-ting, primarily undertaking research on tropical cyclone.
**Corresponding author:** LI Ying, e-mail: yli@cma.gov.cn

favorable time for cyclogenesis in the NIO (Mahala et al. [10]). The intraseasonal oscillation event also influences the formation of tropical cyclones over the NIO within the transition seasons (Yanase et al. [11]; Kikuchi and Wang [12]).

Global warming has affected the frequency and intensity of tropical cyclones. Using cyclone data from a storm atlas issued by the India Meteorological Department for the period 1877–1989, Singh et al. found significant positive trends in the frequency of cyclones with maximum wind speeds >48 kt over the BoB in May and November [13]. However, the frequency of cyclones decreased during the monsoon season (June-September) (Singh [14]; Mandke and Bhide [15]; Vishnu et al. [16]). Mohapatra et al. obtained similar results for tropical cyclones over the BoB in May and November in the time period 1891–1960, but the annual variation in the frequency of tropical cyclones over the BoB in the time period 1961–2008 showed a decreasing trend [17]. Rameshkumar and Sankar explained that warm sea surface temperatures (SSTs) were insufficient for the initiation of convective systems over the BoB [18]. Balagutru et al. indicated that the intensity of strong storms (hurricane categories 3–5) in the post-monsoon period over the BoB increased during the time period 1981–2010 [19]. Rao et al. and Krishna both found that the upper-level tropical easterly jet during the SW monsoon over the NIO has weakened in recent years [20-21]. If this trend continues, it may induce more intense tropical cyclones during the SW monsoon. Evan and Camargo showed that tropical cyclones have intensified over the Arabian Sea in May-June since 1997 [22]. Evan et al. attributed this to significant reductions in the ambient vertical wind shear (VWS) in the troposphere caused by the dimming effects of increased anthropogenic black carbon and other aerosols [23]. Wang et al. showed that the intensification of tropical cyclones in the Arabian Sea in May-June is caused by the substantial advancement (by 15 days) of the occurrence of tropical cyclones caused by the early onset of the Asian SW monsoon [24]. Recent studies have highlighted the importance of the influence of the El Niño-Southern Oscillation on tropical cyclone activity over the BoB by forcing convection, low-level cyclonic vorticity and the heat potential of tropical cyclones (Mahala et al.[10]; Girishkumar and Ravichandran [25]; Felton et al. [26]). Severe tropical cyclones have often occurred over the NIO in recent years, such as Sidr in 2007, Giri in 2010, Phailin in 2013 over the BoB and Chapala in 2015 over the Arabian Sea, all with a maximum wind speed >130 kt (66.9 m $s^{-1}$). Phailin was the strongest tropical cyclone in the world in 2013.

The activities of tropical cyclones in the two seas of the NIO have different patterns and are experiencing temporal changes. Previous climatological studies focused on the activity of tropical cyclones over the entire NIO basin or in only a single sea area; few considered the size and asymmetrical structure of tropical cyclones in both seas. We carried out a comparative statistical analysis of the activities, environmental conditions and wind structure of tropical cyclones over the Arabian Sea and BoB based on the latest and relatively long-term best-track data.

Section 2 describes the data used in this study. Section 3 discusses the activity of tropical cyclones and their different features in the Arabian Sea and BoB. Section 4 investigates the wind structural characteristics of tropical cyclones in the two sea areas by analyzing the size and asymmetrical structure. Section 5 examines the environmental conditions in an attempt to understand the generation features and the differences of tropical cyclones in the two seas.

## 2 DATA AND METHODS

The Joint Typhoon Warning Center (JTWC) provides historical best-track information over the NIO from 1945 to 2018. Using these data, Duan et al. found that there was a sudden change in the frequency of tropical cyclones over the NIO during the mid to late 1970s, from an annual average of 12.4 in the time period 1945–1976 to 3.7 in 1977–2006 [27]. This change may be related to the inconsistencies in observational methods (Mandke and Bhude [15]). After the 1970s, more reliable meteorological satellites and radar systems were used to monitor tropical cyclone activity and their intensity was estimated with the Dvorak model (Chu et al. [28]; Dvorak [29]). The quality of the historical data provided by the India Meteorological Department and the JTWC has been discussed (Evan and Camargo [22]; Zhang et al. [30]). They showed that the India Meteorological Department dataset has a much shorter time period, beginning in 1990, and has irregular time intervals, mainly 3 h, but also 6, 9, 12 and 15 h intervals. By contrast, the JTWC dataset is of good quality, with a longer duration and more stable records estimated every 6 h. We therefore used the tropical cyclone best-track data from 1977 to 2018 and the wind radii information from 2001 to 2018 issued by the JTWC. In addition, the monthly mean reanalysis data at a resolution of 2.5° × 2.5° provided by the National Centers for Environmental Prediction / National Center for Atmospheric Research (NCEP / NCAR) were also used to investigate the background environmental circulation (Kalnay [31]).

The JTWC best-track data include the serial number of the tropical cyclone, its name, time (0000, 0600, 1200 and 1800 GMT), center location, the maximum 1-min sustained wind speed near the center ($V_{max}$, units: knots, where 1 kt=0.514 m $s^{-1}$), the intensity grade, the specified wind (34, 50 and 64 kt) radii in four quadrants, i.e., northeast (NE), southeast (SE), southwest (SW) and northwest (NW), the radius of the maximum wind speed and the radius of the last closed isobar. Based on $V_{max}$, the intensity grade is classified into seven levels by the JTWC criteria: tropical depression, $V_{max}$ <

34 kt (<17.5 m $s^{-1}$); tropical storm, $V_{max}$ 34–63 kt (17.5–32.4 m $s^{-1}$); hurricane category 1 (H1), $V_{max}$ 64–82 kt (32.9–42.2 m $s^{-1}$); hurricane category 2 (H2), $V_{max}$ 83–95 kt (42.7–48.9 m $s^{-1}$); hurricane category 3 (H3), $V_{max}$ 96–112 kt (49.4–57.6 m $s^{-1}$); hurricane category 4 (H4), $V_{max}$ 113–135 kt (58.1–69.4 m $s^{-1}$); and hurricane category 5 (H5), $V_{max}$ >135 kt (>69.4 m $s^{-1}$).

The definition of tropical cyclones in this study are samples which exhibit wind speeds in excess of 17 kt in the NIO. The four tropical cyclones for which the $V_{max}$ value was not estimated are not included in the statistical samples. The genesis points are defined as the location at which a disturbance was first classified as a tropical depression with $V_{max}$ >17 kt in the NIO, which is consistent with previous studies (Kikuchi and Wang [12]; Evan and Camargo [22]; Molinari and Vollaro [32]; Frank and Roundy [33]). We define the duration of the tropical cyclone as the total time for which $V_{max}$ >17 kt and the average duration of tropical cyclones is obtained by dividing the sum of the duration per year by the annual frequency of tropical cyclones. With reference to Ng and Chan, 80° E is taken as the boundary between the Arabian Sea and the BoB [34]. Tropical cyclones generated in the region (0–25° N, 50–80° E) are defined as Arabian Sea tropical cyclones, whereas those generated in the region (0–25° N, 80–110° E) are classified as BoB tropical cyclones. The BoB tropical cyclones include a few that originated from the Indochina Peninsula or the Gulf of Thailand and subsequently entered the BoB.

We use the asymmetric index $\alpha$ defined by Song and Klotzbach to quantitatively evaluate the asymmetry of tropical cyclones:

$$\alpha=\frac{1}{2}\sqrt{(R_{NE}-R_{SW})^2+(R_{SE}-R_{NW})^2} \quad (1)$$

where $R_{NE}$, $R_{SW}$, $R_{SE}$ and $R_{NW}$ refer to the 34 kt wind radii in the NE, SW, SE and NW quadrants, respectively [35]. When the wind field of the tropical cyclone is perfectly symmetrical, $\alpha$ will be zero. Otherwise, a non-zero value of $\alpha$ indicates asymmetry and the direction of the longest radius $\theta$ is estimated as follows:

$$\theta=\arctan\left(\frac{R_{NE}-R_{SE}-R_{SW}+R_{NW}}{R_{NE}+R_{SE}-R_{SW}-R_{NW}}\right) \quad (2)$$

where $\theta$ is categorized by its value in the nearest eight directions: east (0°), NE, north (90°), NW, west (180°), SW, south (270° or −90°) and SE.

The significance of the time series trends is tested using the non-parametric Mann-Kendall test (Kendall [36]). The main advantage of this method is that the sample does not need to obey a certain distribution and a few outliers can be tolerated. It is therefore suitable for non-normally distributed data, as found in meteorology and hydrology, and is easy to calculate.

## 3 ACTIVITY OF TROPICAL CYCLONES OVER THE NIO

### 3.1 *Temporal variation*

#### 3.1.1 ANNUAL VARIATION

During the time period 1977–2018, the total number of tropical cyclones (including tropical depressions) generated in the NIO was 215. Among them, 65 tropical cyclones formed in the Arabian Sea, with an annual average number of 1.6, accounting for about 30% of the total tropical cyclones in the NIO. A total of 150 tropical cyclones were generated in the BoB, accounting for about 70% of the total tropical cyclones in the NIO. The average annual frequency of tropical cyclones in the BoB was 3.6, close to the 3.7 counted by Duan et al. [27].

The mean duration of tropical cyclones in the Arabian Sea was 116 h (about 4.8 days) and showed a significant increasing annual trend (Fig. 1b). The shortest tropical cyclone of only 36 h occurred in 1983, whereas the longest of 276 h (11.5 days) occurred in 1997. The mean duration of tropical cyclones in the BoB was 128 h (5.3 days) and showed a slight negative annual trend. The shortest tropical cyclone of only 12 h occurred in 1986, whereas the longest of 462 h (19 days) occurred in 1996.

The frequency of occurrence of tropical cyclones shows a clear increasing trend in the Arabian Sea (Fig. 1a), statistically significant at the 95% level, and is consistent with the findings of Zhang et al. [30]. Fig. 1c shows that this increasing trend is mainly due to the increase in the number of H1–H5 grade cyclones, consistent with the results of Webster et al. [37]. There was only one tropical depression in the Arabian Sea (not shown in Fig. 1c). The frequency of occurrence of tropical cyclones in the BoB has decreased, but not significantly, consistent with the findings of Mohapatra et al. [17]. However, there is no clear change in stronger cyclones (H1–H5 grades), whereas the number of tropical depressions has decreased (Fig. 1d).

The MeteoSat-5 satellite was relocated from 8 to 63.8° E in 1998 and 3-h satellite observations in the infrared and visible channels were established directly over the Arabian Sea (Knapp and Kossin [38]), which is likely to result in a different estimation of intensity from that in the JTWC database. The change in the frequency of tropical cyclones in different categories of intensity is therefore uncertain. Based on a homogenous reanalysis of satellite imagery, some studies demonstrated that there has been no trend toward an increase in the number of H3–H5 cyclones over the NIO from 1980 to 2009 (Landsea [39]; Kossin et al. [40]; Hoarau et al. [41]). In view of the uncertain influence of tropical depressions, we re-counted the annual variation in the frequency and duration of the samples without tropical depressions and confirm our earlier conclusions.

This analysis shows that the frequency and duration of tropical cyclones have a significant increasing trend (> 95% confidence level) in the Arabian Sea, but not in the BoB. This may be related to the abrupt interdecadal change in the SW monsoon circulation in South Asia.

Xiang and Wang showed that the onset of the Asian summer monsoon in May has advanced remarkably since 1999, leading to the earlier genesis of tropical cyclones over the Arabian Sea and an increase in the frequency and duration of tropical cyclones [42]. May is the normal genesis time of tropical cyclones over the BoB, leading to few significant change over the number of tropical cyclones over the BoB.

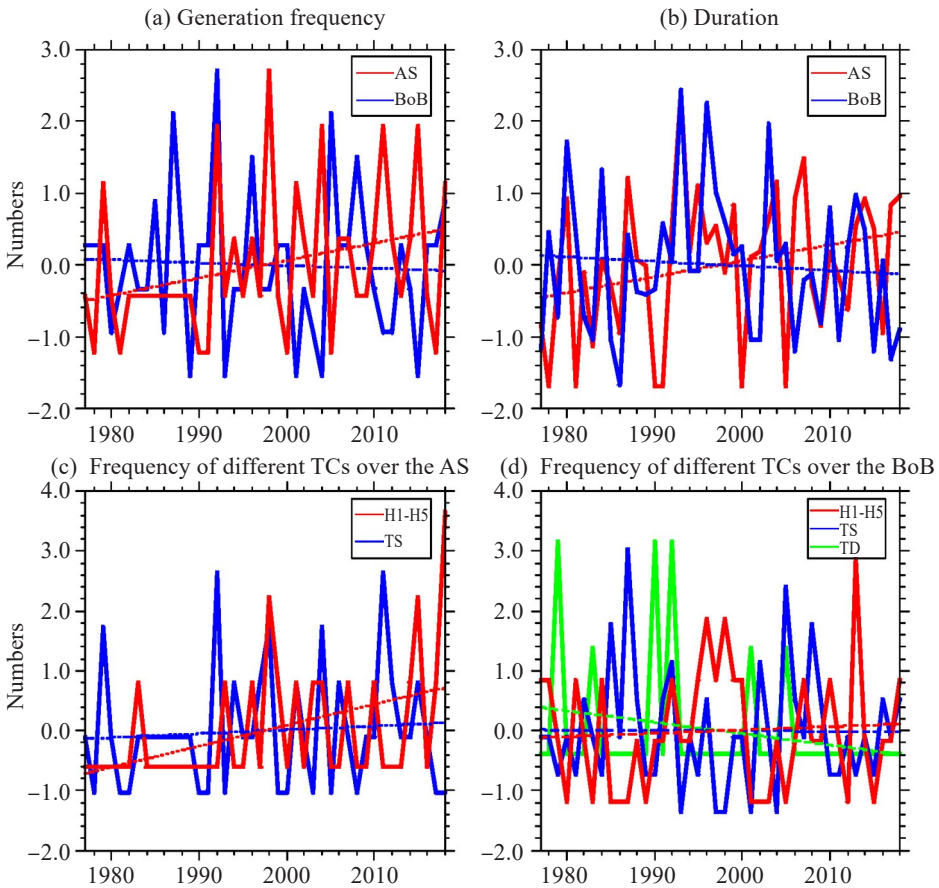


**Figure 1.** Annual variation of (a) the number and (b) the average duration of tropical cyclones (TC) after *z*-score standardization over the Arabian Sea (AS, red lines) and Bay of Bengal (BoB, blue lines) during the time period 1977–2018. Annual variation in the frequencies of TC of different intensity grades in the (c) AS and (d) BoB, including tropical depressions (TD, green lines), tropical storms (TS, blue lines) and hurricane grades H1–H5 (red lines) after *z*-score standardization. The dotted lines indicate the trends.

### 3.1.2 MONTHLY VARIATIONS

Figure 2 shows the monthly occurrence number of tropical cyclones over the NIO during the time period 1977–2018. There was no tropical cyclone over the Arabian Sea in January-April and July (Fig 2a) and no tropical cyclone over the BoB (Fig. 2b) in February and August. The monthly frequencies of tropical cyclones in both basins show a clear bimodal character. The first peak in the Arabian Sea occurs in May (12 tropical cyclones) and then in June (14 tropical cyclones). June is the only month in which there are more tropical cyclones over the Arabian Sea than over the BoB. The second peak is in November, with a total of 17 tropical cyclones, and ends in December. The largest proportion (about 50%) of strong cyclones (H1–H5 grades) in the Arabian Sea occurs in May. Tropical cyclones seldom occur consecutively over the Arabian Sea in May and June (except in 1998) and in October and November (except in 2015). This pattern is associated with the onset and withdrawal of the transition season for monsoons over the Arabian Sea. Evan and Camargo suggested that May (June) storms over the Arabian Sea are related to an early (late) onset of the SW monsoon [22]. The first peak in the BoB occurs in May, with a total of 23 tropical cyclones. The maximum peak in the BoB occurs in November, with a total of 39 tropical cyclones, and then a secondary peak of 37 in October. The largest proportion of strong cyclones (about 62.5%) occurs in April. The number of tropical cyclones over both seas shows a bimodal distribution, with the maximum peak occurring in autumn (November) and a larger proportion of stronger tropical cyclones occurring in early summer (April or May). The tropical cyclones over the Arabian Sea break out later in early summer and end earlier in the autumn than those in the BoB.

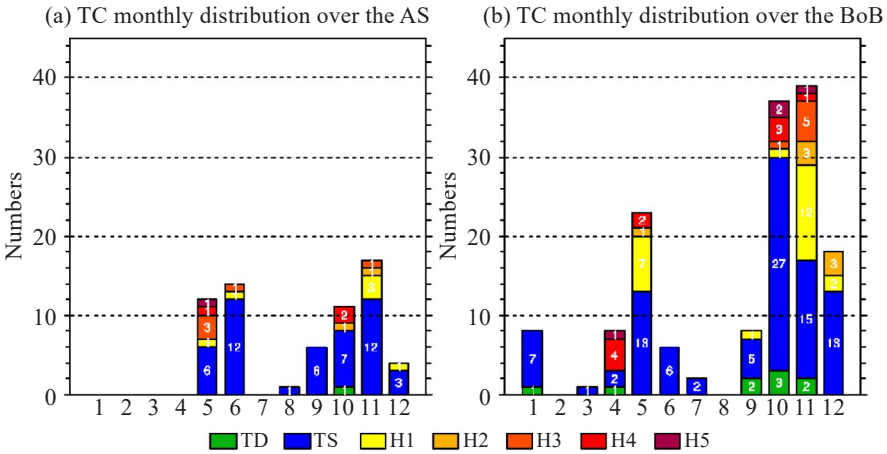


**Figure 2.** Monthly numbers of TC with different intensity grades in the (a) AS and (b) BoB. The climatology period is 1977–2018.

### 3.2 *Geographical distribution*

#### 3.2.1 TROPICAL CYCLONE TRACKS

The movements of tropical cyclones show three different types of tracks: NW, NE and west (Fig. 3). The classification standard for the track of tropical cyclones is adopted according to the first landfall location, or the point of final disappearance for tropical cyclones that do not make landfall. Tropical cyclones over the Arabian Sea with landfall/disappearance points located north of 15° N and west of 60° E are defined as the NW track, those north of 15° N and east of 60° E are defined as the NE track and those south of 15° N and west of 60° E are defined as the westward track. Tropical cyclones over the BoB with landfall/disappearance points located north of 15° N and west of 90° E or north of 20° N are defined as the NW track, those in the region 15–20° N and east of 90° E are defined as the NE track and those south of 15° N and west of 90° E are defined as the westward track (Duan et al. [27]).

Tropical cyclones over the Arabian Sea tend to move westward at lower latitudes. Although most of the tropical cyclones moved NW along the Western Ghats at slightly higher latitudes, some turned to the NE around 15° N and then made landfall in southern Pakistan or the NW corner of the Indian Peninsula. The westward track accounts for the highest proportion (37.3%) of tropical cyclones in the Arabian Sea, followed by the NW track (34.3%), whereas the NE track accounts for the lowest proportion with 25.4%. The proportions of the three types of tracks are similar in the BoB, with each accounting for about one-third of the total. Among them, tropical cyclones with NW and NE tracks may affect precipitation in the southwestern and plateau regions of China (Xiao and Duan [43]). Only three tropical cyclones moved into Yunnan Province (in April 1991, May 1992 and October 2010). Tropical cyclones in the BoB with a westward track mainly affect southeastern India and Sri Lanka; about 39% of these tropical cyclones can move westward into the Arabian Sea and may make landfall for a second time.

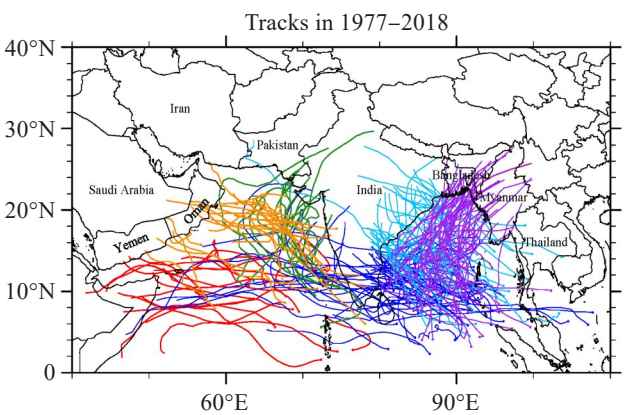


**Figure 3.** Regional distribution of TC tracks in the AS and BoB during the time period 1977–2018. In the AS, the green, orange and red lines represent the NE, NW and westward tracks, respectively. In the BoB, the purple, light blue and dark blue lines represent the NE, NW and westward tracks, respectively.

#### 3.2.2 TROPICAL CYCLONE OCCURRENCE FREQUENCY AND AVERAGE INTENSITY

Figure 4 shows the 2.5°×2.5° rasterized distribution of the occurrence frequency of tropical cyclones at 6 h intervals and their average $V_{max}$ over the NIO during the time period 1977–2018. The area with most samples mainly covers (10–20° N, 60–70° E) over the Arabian Sea and (8–20° N, 80–90° E) over the BoB, with the large value centers located in the SE and NW of their respective sea areas. The spatial distribution of the grids with an average $V_{max}$ >25 m s$^{-1}$ (red grids) over the Arabian Sea is mainly distributed near 60° E and the west coast. This distribution is significantly broader than that over the BoB, where tropical cyclones only occur in the northern triangular region near the coast. The feature indicates that there are more strong tropical cyclones over the Arabian Sea than over the BoB.

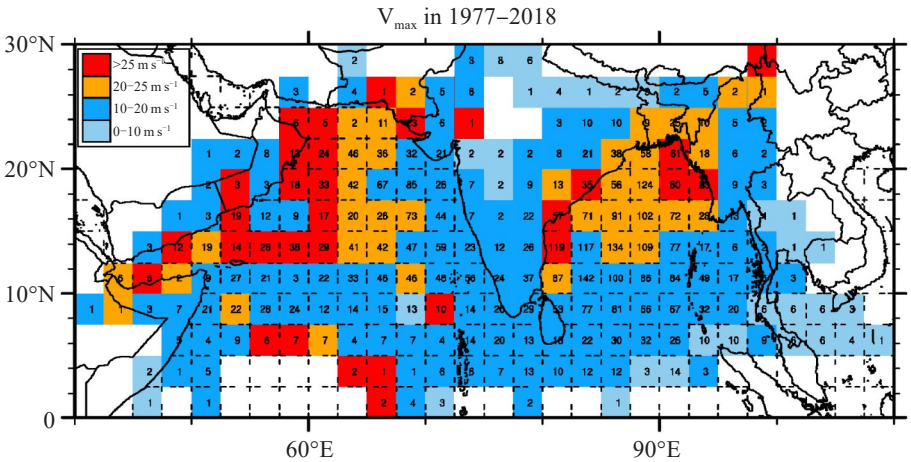


**Figure 4.** Regional distribution of the frequency of TC (numbers in the grid) at 6-h intervals over the North Indian Ocean (NIO) and the sample-averaged value of the maximum sustained wind speed ($V_{max}$, shaded grids; units: m s$^{-1}$) during the time period 1977–2018. The grid size is 2.5°×2.5°.

## 4 STRUCTURAL CHARACTERISTICS OF WINDS

### 4.1 *Radius of maximum wind*

The radius of maximum wind (RMW) of tropical cyclones over the NIO is recorded every 6 h. The total number of samples during the time period 2001–2018 is 2011, including 778 over the Arabian Sea and 1233 over the BoB. Fig. 5 shows the frequency distribution of the RMW; the six samples in the BoB with RMW >150 km are not shown. Most of the tropical cyclones have an RMW between 15 and 90 km, accounting for about 79% of tropical cyclones over the Arabian Sea and 88% over the BoB. The mean value of the RMW over the Arabian Sea (BoB) is 51 (55) km and the RMW with the most samples is 28 (74) km, indicating that the RMW over the Arabian Sea is smaller than that over the BoB.

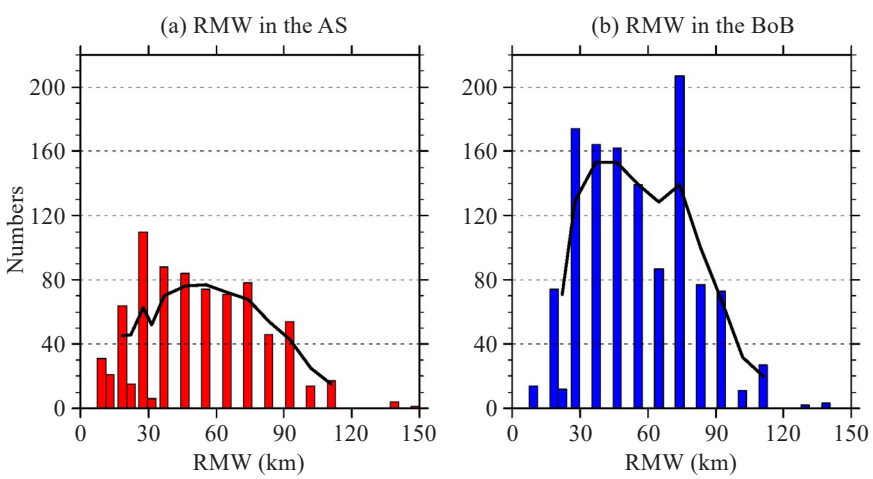


**Figure 5.** Frequency distribution of the radius of maximum wind (RMW) of TC over the (a) AS and (b) BoB from 2001 to 2018.

### 4.2 *34 kt wind radii ($R_{34}$)*

There were 885 tropical cyclones over the NIO from 2001 to 2018 based on the 34 kt wind radii ($R_{34}$) measured at 6 h intervals. The shape parameters of the 34 kt surface wind of tropical cyclones over the Arabian Sea and BoB are mostly in the NE quadrant—that is, the gale mainly appears in the NE quadrant of the tropical cyclone circulation. The size of a tropical cyclone is defined as the azimuthal mean radius of the 34 kt surface wind (Lu et al. [44]). Tropical cyclones over the NIO have an average size of 139 km, which is much smaller than that of tropical cyclones over the western North Pacific, which have an average size of 203 km (Lu et al. [44]). The mean sizes of tropical cyclones over the Arabian Sea and the BoB are 146 and 135 km, respectively. Table 1 gives the mean and maximum size in different intensity and seasonal groups and shows that strong cyclones are larger than tropical storms in both seas, consistent with the results of Mohapatra and Sharma—that is, the size (34 kt) of tropical cyclones in the Arabian Sea and BoB increases significantly with the increase in the intensity of the tropical cyclone [45]. The size of tropical cyclones

in the NIO in early summer is larger than that in autumn, especially in the Arabian Sea.

Figure 6 shows the regional distribution of the size of tropical cyclones over the NIO on 2.5°×2.5° grids and suggests that the maximum value of the mean size can reach more than 200 km (red grids) in both sea areas, although the number of samples is small. More than half the grids in the Arabian Sea have tropical cyclones with a mean size >150 km (orange and red grids), mainly distributed in the western basin. In the BoB, the most frequent size of tropical cyclones is 100–150 km (yellow grids) and grids with a mean size >150 km (orange and red grids) are only located in the area north of 15° N. This shows that the size of tropical cyclones in the Arabian Sea are generally larger than those in the BoB.

**Table 1.** Size of tropical cyclones in groups of different intensity and different seasons.

| | Intensity grade over the Arabian Sea (BoB) | | Time period over the Arabian Sea (BoB) | |
|---|---|---|---|---|
| | Tropical storm | H1–H5 | May–June | October–December |
| Average size (km) | 127 (122) | 186 (172) | 153 (140) | 144 (136) |
| Maximum size (km) | 248 (257) | 329 (310) | 329 (310) | 250 (269) |
| Minimum size (km) | 35 (19) | 72 (83) | 56 (19) | 35 (37) |
| Sample size | 252 (388) | 115 (134) | 141 (135) | 211 (325) |

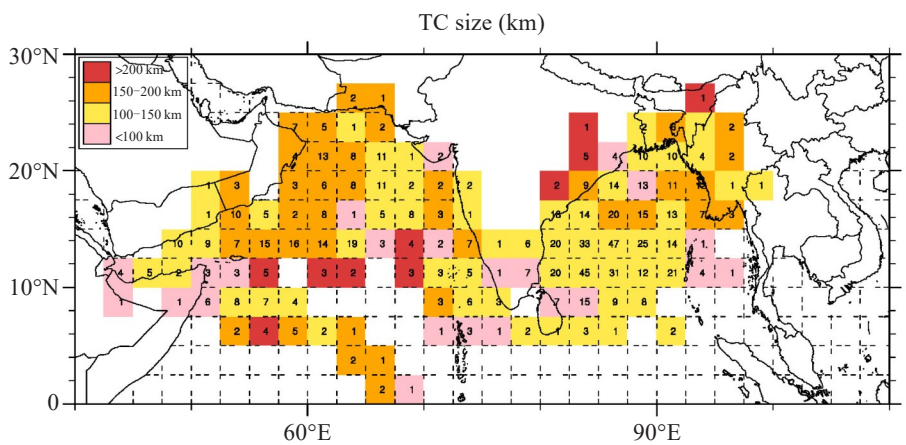


**Figure 6.** Regional distribution of the size of TC (units: km) over the NIO from 2001 to 2018. The grid size is 2.5°×2.5°. The number in each grid is the number of samples.

There are some differences in the wind radii in different quadrants of the tropical cyclones. The mean value of $R_{34}$ over the SW, NW, NE and SE quadrants of tropical cyclones over the Arabian Sea (BoB) are 145 (130), 148 (129), 151 (136) and 152 (137) km, respectively. On average, $R_{34}$ is larger over the Arabian Sea than over the BoB in all four quadrants and the wind radius is larger in the eastern quadrants (NE, SE) than in the western quadrants (NW, SW) in both seas.

Figure 7a and 7b show the frequency of $R_{34}$ in the four quadrants of tropical cyclones over the Arabian Sea and BoB, respectively. The number of tropical cyclone samples with $R_{34}$ between 100 and 150 km is highest in both basins, although there are differences between the four quadrants. The proportion of samples with $R_{34}$ <150 km is greater in the BoB than in the Arabian Sea. Taking the NE quadrant as an example, samples with $R_{34}$ <150 km account for 58 (69)% of the total samples over the Arabian Sea (BoB). The number of samples with $R_{34}$ between 200 and 250 km over the Arabian Sea and $R_{34}$ > 250 km over the BoB shows that the eastern quadrants have a higher frequency of tropical cyclones than the western quadrants do, whereas the number of samples with $R_{34}$ between 50 and 100 km is significantly greater in the western quadrants than in the eastern quadrants in both basins. This shows the asymmetrical structure of tropical cyclones over the NIO, with large (small) values of $R_{34}$ occurring mainly in the eastern (western) quadrants.

### 4.3 *Asymmetrical structure*

The asymmetry index ($\alpha$) and the direction of the longest radius ($\theta$) of tropical cyclones over the NIO from 2001 to 2018 show that the mean values of $\alpha$ in the Arabian Sea and BoB are 19.69 and 20.85 km, respectively, and $\alpha$ can reach up to 40 km in both seas (Fig. 8). The regions with significant asymmetry in the Arabian Sea are mainly located on the SW coast of the Indian Peninsula and the east coast of the Arabian

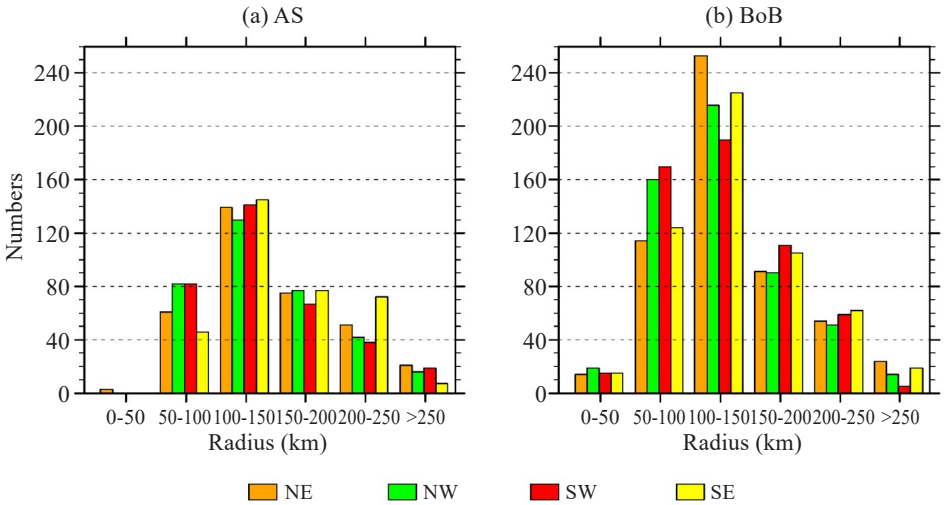


**Figure 7.** Frequency distribution of the 34 kt wind radii ($R_{34}$) in the NE (orange), NW (green), SW (red) and SE (yellow) quadrants over the (a) AS and (b) BoB. The horizontal axis represents the radius (units: km) and the vertical axis is the frequency.

Peninsula, whereas the asymmetry in the central basin is weak. In the BoB, the grids with $\alpha$ >20 (30) km are located north of 10° N (20° N) and the asymmetry is strong where the tropical cyclone makes landfall, especially in the eastern part of the Indian Peninsula and the coastline of Myanmar and Bangladesh. This shows the influence of terrain on the asymmetrical structure of tropical cyclones over the NIO.

The value of $\theta$ is between −90 and +90° in both seas—that is, the longest radius of the 34 kt surface wind is located in the eastern quadrants of the tropical cyclone circulation. The value of $\theta$ in the central basin of the Arabian Sea is mostly positive, which means that the longest radius is in the NE quadrant, whereas the longest radius in the coastal areas is often in the SE quadrant ($\theta$ <0). The longest radius in the BoB is mostly in the NE quadrant ($\theta$ >0) if the samples make landfall on the peninsula of India and north of 20° N, whereas it is always in the SE quadrant ($\theta$ <0) when the samples are located in the central basin.

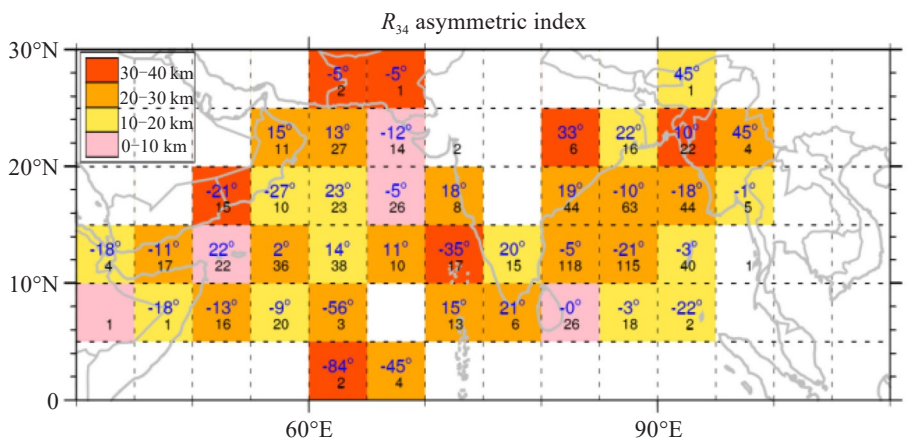


**Figure 8.** Distribution of the asymmetry of TC over the NIO from 2001 to 2018. The shaded grid indicates the distribution of the asymmetry index $\alpha$ (units: km) of $R_{34}$. The grid size is 5°×5°. The black number in each grid indicates the sample size and the blue number is the direction of the longest radius $\theta$ (units: °) of $R_{34}$.

## 5 CAUSE OF THE DIFFERENCE IN TROPICAL CYCLONE ACTIVITY IN THE TWO SEAS

Previous studies have suggested that large-scale environmental parameters, such as the SST, low-level vorticity, mid-tropospheric humidity and VWS, influence the genesis and development of storms over the NIO (Pattanaik [5]; Rameshkumar and Sankar [18]; Evan and Camargo [22]).

Figure 9 shows the distribution of the relative vorticity (shaded) at 850 hPa and the genesis points (dots) of tropical cyclones in the NIO for each month. In the Arabian Sea, tropical cyclones are mainly generated in the eastern basin. From January to April (Fig. 9a-d), the region of positive vorticity is located south of 10° N

over the NIO, with larger values in the BoB. A few tropical cyclones occur in the south of the BoB in January and April, but no tropical cyclone is found over the Arabian Sea as a result of the control by the Iranian subtropical high. In May (Fig. 9e), with the cross-equatorial flow extending northward into the NIO, the SW monsoon is observed in both sea areas with a positive vorticity belt, especially in the BoB. The SW monsoon and positive vorticity are stronger and move northward in June (Fig. 9f). Tropical cyclones in the BoB originate in a southwesterly flow and present a meridional distribution in May and June. The southwesterly low-level jet is then enhanced, with the maximum value of positive vorticity in July and August (Fig. 9g and 9h). However, only three tropical cyclones are generated in the NIO as a result of restriction by the large VWS. When the SW monsoon weakens and retreats toward the equator, the region of positive vorticity and the points of genesis of tropical cyclones in the BoB also move south in a zonal distribution from September to December (Fig. 9i-l). The time of onset (drawback) of the SW monsoon over the Arabian Sea is usually later (earlier) than that over the BoB and therefore the time of tropical cyclone outbreak (end) over the Arabian Sea is later (earlier) than over the BoB.

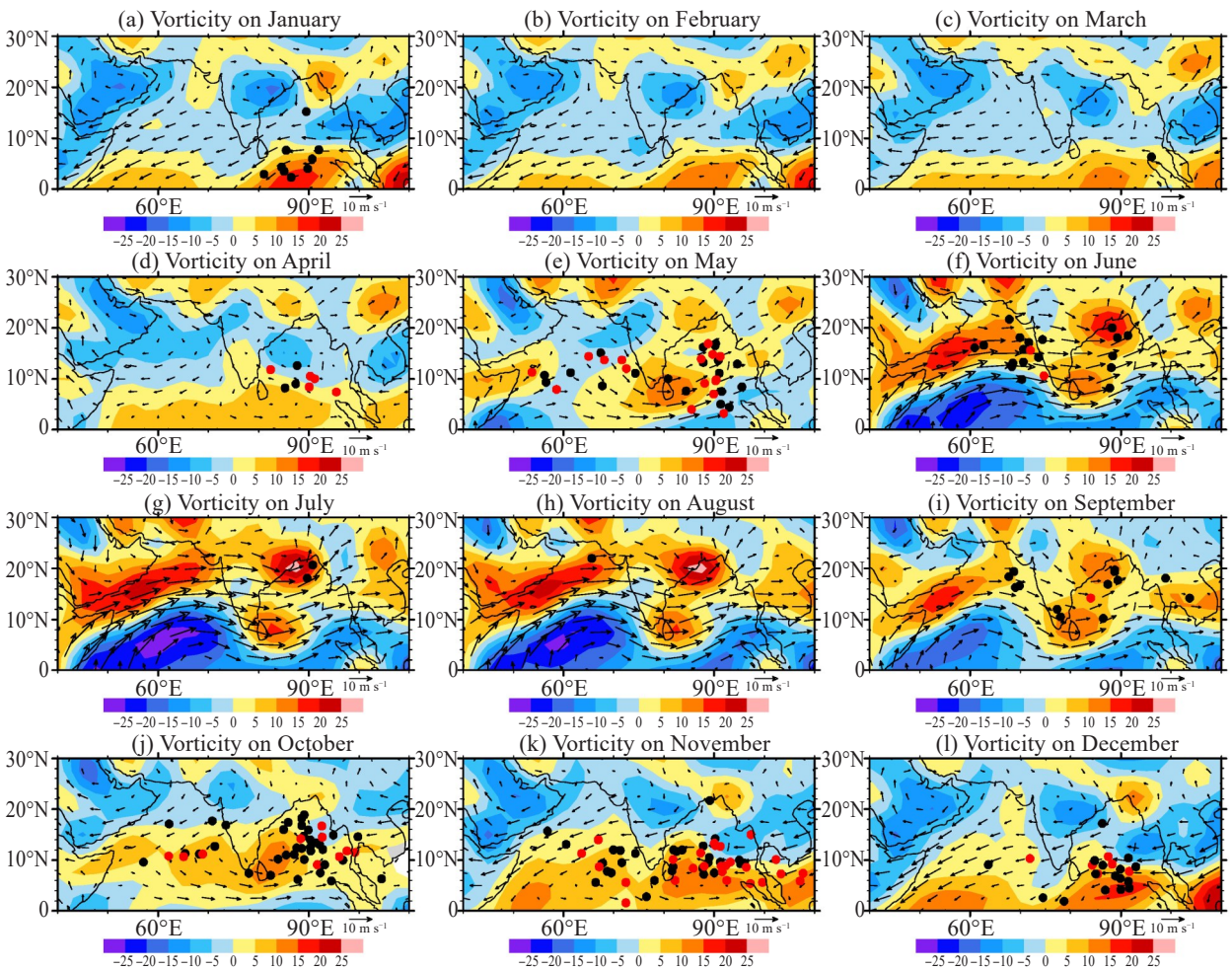


**Figure 9.** Distribution of the monthly mean 850 hPa relative vorticity (shading; units: $10^{-7}$ $s^{-1}$) and 850 hPa vector winds (arrows; units: m $s^{-1}$) from January to December. The climatology period is 1977–2018 and the red (black) dots represent locations of genesis of hurricane grades H1–H5 (TD and TS) for each month.

The seasonal pattern of the development of cyclones over the NIO is related to the annual cycle of the VWS, which is defined as the difference in wind speed between the 200 and 850 hPa layers. The monthly mean distribution of VWS over the NIO (Fig. 10) indicates that the Qinghai-Tibetan Plateau is controlled by the South Asian high in June-September and the NIO is controlled by the easterly high-level jet at 200 hPa. This leads to a large VWS between the high-level jet and the southwesterly jet in the lower layer, which may limit the formation of tropical cyclones. The few tropical cyclones that occur during this season are concentrated in the northern basins where the VWS is weak. By contrast, the South Asian high in the upper troposphere generally moves away from the Qinghai-Tibetan Plateau during January-May and October-December and the westerly jet prevails over the NIO, leading to a weak VWS and providing favorable conditions for the

generation of tropical cyclones.

The SST and relative humidity also affect the activity of tropical cyclones over the NIO. Warm water with an SST >26° C is recognized as a necessary condition for the formation of tropical cyclones (Gary [2]). The SST is the highest (>30°C) in the NIO in April-May (figure omitted), which may explain why stronger cyclones are likely to occur in April over the BoB and in May over the Arabian Sea. By contrast, the mean relative humidity is different in the NIO between the two peak periods. The mean value of relative humidity at 600 hPa in the key area of the points of tropical cyclone genesis over the NIO is 36% in May and 48% in November during the time period 1977–2018, which favors the generation of tropical cyclones in the autumn months (Li et al. [4]).

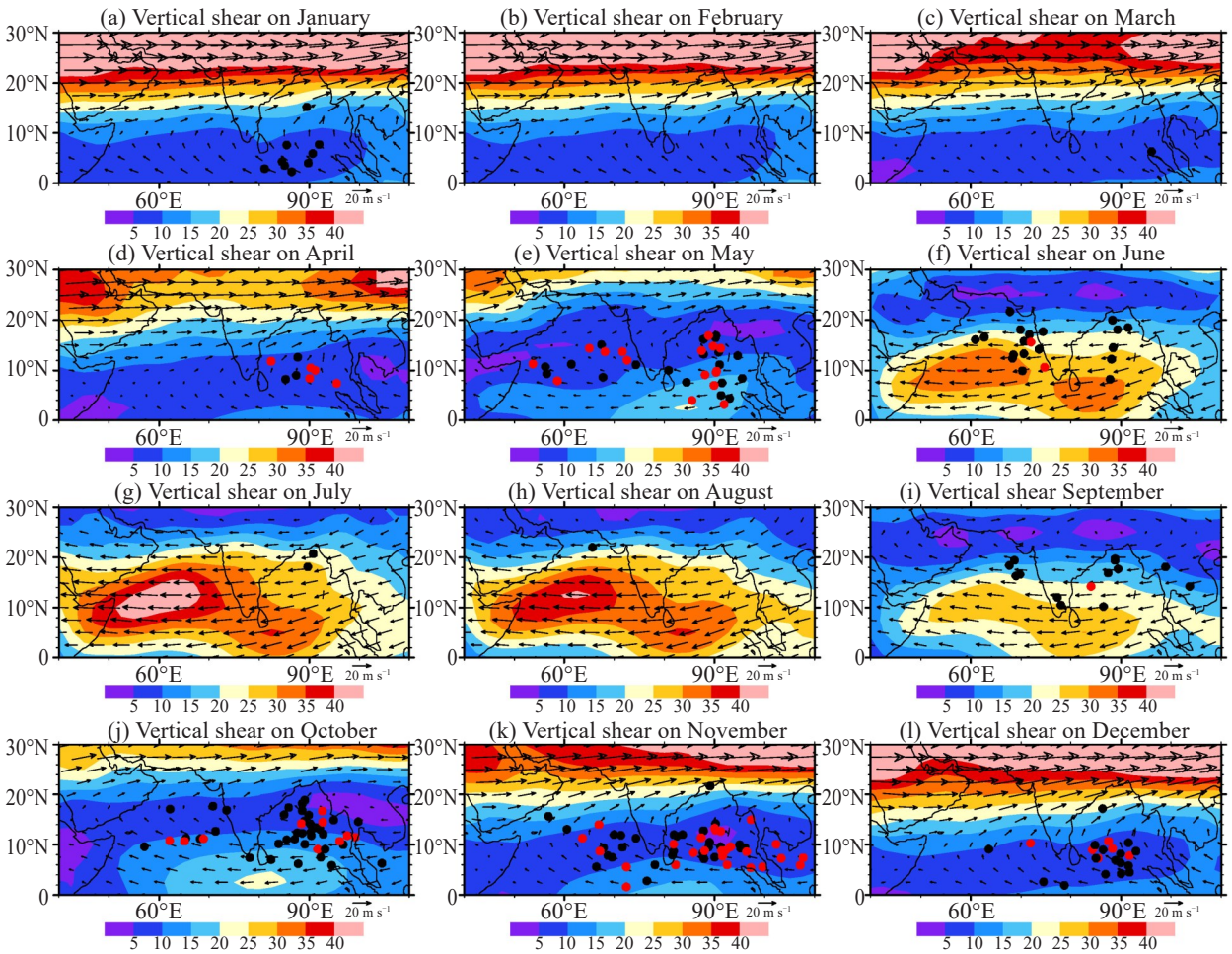


**Figure 10.** As in Fig. 9 but for monthly mean vertical wind shear (shading; units: m $s^{-1}$) and 200 hPa vector winds (arrows; units: m $s^{-1}$).

## 6 SUMMARY AND CONCLUSIONS

We carried out a comparative analysis of the activity characteristics, environmental conditions, size and wind structural features of tropical cyclones over the Arabian Sea and BoB based on the JTWC best-track data from 1977 to 2018 and the monthly mean reanalysis data provided by NCEP/NCAR. Our conclusions are as follows.

(1) About 30% of the tropical cyclones over the NIO are active over the Arabian Sea and 70% over the BoB. The annual generation frequency of tropical cyclones over the Arabian Sea has a significant increasing trend, whereas an insignificant deceasing trend is observed for tropical cyclones over the BoB. The monthly frequency of tropical cyclones over both seas has a notable bimodal character. More tropical cyclones occur in autumn as a result of the higher moisture content at mid-levels, whereas the proportion of strong cyclones is greater in April-May as a result of the higher SST. Tropical cyclones in the Arabian Sea break out later during the first peak and end earlier during the second peak than those in the BoB, which is attributed to the activity of the SW monsoon in the NIO.

(2) Tropical cyclones over the Arabian Sea are mainly generated over the eastern basin, whereas the genesis locations of tropical cyclones over the BoB vary with the seasonal movement of the low-level positive vorticity and have a meridional distribution in May-June and a zonal distribution in October-December. Tropical

cyclones with west and the NW tracks are the most common types in the Arabian Sea, accounting for about 74.6%, whereas tropical cyclones with a NE track are the least common. By contrast, the three types of tropical cyclone tracks have similar proportions over the BoB.

(3) The mean intensity and size of tropical cyclones over the Arabian Sea are stronger and larger than those over the BoB and the size of tropical cyclones over the NIO are larger in early summer than in the autumn, especially in the Arabian Sea. The asymmetrical structure of tropical cyclones is greatly affected by topography and tropical cyclones that occur along the peninsula coast are more asymmetrical. The longest radius direction of the 34 kt surface wind is often located in the eastern quadrants of the tropical cyclone circulation in the both sea areas.

The wind radius information used in section 5 was estimated subjectively by the operational forecaster based on all the available observational products at that time, including satellites and coastal radar systems, and then recorded directly in the best-track data of the JTWC dataset without quality control (Chu et al. [28]). However, as a result of difficulties in observing and verifying the tropical cyclone wind field, these data are generally considered to be the best estimate of the true value and have been widely used in studies of the wind structure of tropical cyclones (Lei and Che [46]; Yuan et al. [47]; Yuan et al. [48]). In addition, because the JTWC has only released wind radius data since 2001, the sample size in our analysis is reduced, but it still reflects the size of the tropical cyclone and the wind structure in the two seas and is meaningful in forecasts and assessments of the impact of tropical cyclones over the NIO.

## REFERENCES


[1] RIEHL H. On the formation of typhoons [J]. J Meteor, 1948, 5(6): 247-265, https://doi. org / 10.1175 / 1520-0469 (1948)005<0247:OTFOT>2.0.CO;2.

[2] GRAY W M. Global view of the origin of tropical disturbances and storms [J]. Mon Wea Rev, 1968, 96(10): 669-700, https://doi. org / 10.1175 / 1520-0493(1968)096< 0669:GVOTOO>2.0.CO;2.

[3] CHUTIA L, PATHAK B, PAROTTIL A, et al. Impact of microphysics parameterizations and horizontal resolutions on simulation of "MORA" tropical cyclone over Bay of Bengal using Numerical Weather Prediction Model [J]. Meteor Atmos Phys, 2019, 131(5): 1483-1495, https://doi. org/10.1007/s00703-018-0651-0.

[4] LI Z, YU W, LI T, et al. Bimodal character of cyclone climatology in the Bay of Bengal modulated by monsoon seasonal cycle [J]. J Climate, 2013, 26(3): 1033-1046, https://doi.org/10.1175/JCLI-D-11-00627.1.

[5] PATTANAIK D R. Variability of oceanic and atmospheric conditions during active and inactive periods of storms over the Indian region [J]. Int J Climatol, 2005, 25(11): 1523-1530, https://doi.org/10.1002/joc.1189.

[6] CAMARGO S J, EMANUEL K A, SOBEL A H. Use of a genesis potential index to diagnose ENSO effects on tropical cyclone genesis [J]. J Climate, 2007, 20(19): 4819-4834, https://doi.org/10.1175/JCLI4282.1.

[7] JADHAV S K, MUNOT A A. Warming SST of Bay of Bengal and decrease in formation of cyclonic disturbances over the Indian region during southwest monsoon season [J]. Theor Appl Climatol, 2009, 96(3-4): 327-336, https:// doi.org/10.1007/s00704-008-0043-3.

[8] KRISHNAMURTI T N, KUMAR A, YAP K S, et al. Performance of a high-resolution mesoscale tropical prediction model [J]. Adv Geophys, 1990, 32: 133-286, https://doi.org/10.1016/S0065-2687(08)60428-8.

[9] MAO Jiang-yu, WU Guo-xiong. Barotropic process contributing to the formation and growth of tropical cyclone Nargis [J]. Adv Atmos Sci, 2011, 28(3): 483, https: //doi.org/10.1007/s00376-010-9190-4.

[10] MAHALA B K, NAYAK B K, MOHANTY P K. Impacts of ENSO and IOD on tropical cyclone activity in the Bay of Bengal [J]. Nat Hazards, 2015, 75(2): 1105-1125, https: //doi.org/10.1007/s11069-014-1360-8.

[11] YANASE W, SATOH M, TANIGUCLiHI H, et al. Seasonal and intraseasonal modulation of tropical cyclogenesis environment over the Bay of Bengal during the extended summer monsoon [J]. J Climate, 2012, 25 (8): 2914-2930, https://doi. org / 10.1175 / JCLI-D-11-00208.1.

[12] KIKUCHI K, WANG B. Formation of tropical cyclones in the northern Indian Ocean associated with two types of tropical intraseasonal oscillation modes [J]. J Meteor Soc Japan, 2010, 88(3): 475-496, https://doi. org / 10.2151 / jmsj.2010-313.

[13] SINGH O P, KHAN T M A, RAHMAN M S. Changes in the frequency of tropical cyclones over the North Indian Ocean [J]. Meteor Atmos Phys, 2000, 75(1-2): 11-20, https://doi.org/10.1007/s007030070011.

[14] SINGH O P. Long term trends in the frequency of monsoonal cyclonic disturbances over the North Indian Ocean [J]. Mausam, 2001, 52(4): 655-658.

[15] MANDKE S K, BHIDE U V. A study of decreasing storm frequency over Bay of Bengal [J]. Geophys Union, 2003, 7(2): 53-58.

[16] Vishnu S, Francis P A, Shenoi S S C, et al. On the decreasing trend of the number of monsoon depressions in the Bay of Bengal [J]. Environ Res Lett, 2016, 11(1): 014011, https://doi.org/10.1088/1748-9326/11/1/014011.

[17] MOHAPATRA M, SRIVASTAVA A K, BALACHANDRAN S, et al. Inter-annual variation and trends in Tropical Cyclones and Monsoon Depressions over the North Indian Ocean [M]// Rajeevan M., Nayak S. (eds), Observed Climate Variability and Change over the Indian Region. Singapore: Springer, 2017: 89-106, https:// doi.org/10.1007/978-981-10-2531-0_6.

[18] RAMESHKUMAR M R, SANKAR S. Impact of global warming on cyclonic storms over north Indian Ocean [J]. Indian J Geo-Mar Sci, 2010, 39(4): 516-520, https://doi. org/10.1093/icesjms/fsq153.

[19] BALAGURU K, TARAPHDAR S, LEUNG L R, et al. Increase in the intensity of postmonsoon Bay of Bengal tropical cyclones [J]. Geophys Res Lett, 2014, 41(10): 3594-3601, https://doi.org/10.1002/2014GL060197.

[20] RAO V B, FERREIRA C C, FRANCHITO S H, et al. In a changing climate weakening tropical easterly jet induces

more violent tropical storms over the north Indian Ocean [J]. Geophys Res Lett, 2008, 35(15): L15710, https://doi.org/10.1029/2008GL034729.

[21] KRISHNA K M. Intensifying tropical cyclones over the North Indian Ocean during summer monsoon—global warming [J]. Global Planet Change, 2009, 65(1-2): 12-16, https://doi.org/10.1016/j.gloplacha.2008.10.007.

[22] EVAN A T, CAMARGO S J. A climatology of Arabian Sea cyclonic storms [J]. J Climate, 2011, 24(1): 140-158, https://doi.org/10.1175/2010JCLI3611.1.

[23] EVAN A T, KOSSIN J P, RAMANATHAN V. Arabian Sea tropical cyclones intensified by emissions of black carbon and other aerosols [J]. Nature, 2011, 479(7371): 94-97, https://doi.org/10.1038/nature10552.

[24] WANG B, XU S B, WU L. Intensified Arabian Sea tropical storms [J]. Nature, 2012, 489(7416): E1-E2, https://doi.org/10.1038/nature11470.

[25] GIRISHKUMAR M S, RAVICHANDRAN M. The influences of ENSO on tropical cyclone activity in the Bay of Bengal during October-December [J]. J Geophys Res Ocean, 2012, 117(C2): C02033, https://doi. org / 10.1029/2011JC007417.

[26] FELTON C S, SUBRAHMANYAM B, MURTY V S N. ENSO-modulated cyclogenesis over the Bay of Bengal [J]. J Climate, 2013, 26(24): 9806-9818, https://doi. org / 10.1175/JCLI-D-13-00134.1.

[27] DUAN Xu, TAO Yun, CUN Can-qiong, et al. Temporal and spatial distributions of storms over the Bay of Bengal and its activity characteristic [J]. Plateau Meteorol, 2009, 28(3): 634-641(in Chinese), https://doi. org / 10.1016 / S1003-6326(09)60084-4..

[28] CHU J H, SAMPSON C R, LEVINE A S, et al. The Joint Typhoon Warning Center Tropical Cyclone Best-Tracks [R]. Technical report, Ref NRL/MR/7540-02, 2002, 16.

[29] DVORAK V F. Tropical cyclone intensity analysis and forecasting from satellite imagery [J]. Mon Wea Rev, 1975, 103(5): 420-430, https://doi.org/10.1175/1520-0493(1975)103<0420:TCIAAF>2.0.CO;2.

[30] ZHANG Fei, WU Li-guang, REN Fu-min, et al. Differences of bimode patterns in TC activity and the possible causes in the Bay of Bengal and the Arabian Sea [J]. J Trop Meteor, 2016, 32(3): 399-406, https://doi.org/10.16032/j.issn.1004-4965.2016.03.011. (in Chinese).

[31] KALNAY. The NCEP / NCAR 40-year reanalysis project [J]. Bull Am Meteorol Soc, 1996, 77(3): 437-472, https://doi.org/10.1175/1520-0477(1996)077<0437:TNYRP>2.0.CO;2.

[32] MOLINARI J, VOLLARO D. Planetary-and synoptic-scale influences on eastern Pacific tropical cyclogenesis [J]. Mon Wea Rev, 2000, 128(9): 3296-3307, https://doi.org/10.1175/1520-0493(2000)128<3296:PASSIO>2.0.CO;2.

[33] FRANK W M, ROUNDY P E. The role of tropical waves in tropical cyclogenesis [J]. Mon Wea Rev, 2006, 134(9): 2397-2417, https://doi.org/10.1175/MWR3204.1.

[34] NG E K W, CHAN J C L. Interannual variations of tropical cyclone activity over the north Indian Ocean [J]. Int J Climatol, 2012, 32(6): 819-830, https://doi. org / 10.1002/joc.2304.

[35] SONG J, KLOTZBACH P J. Wind structure discrepancies between two best track datasets for western north Pacific tropical cyclones [J]. Mon Wea Rev, 2016, 144(12): 4533-4551, https://doi.org/10.1175/MWR-D-16-0163.1.

[36] Kendall M G. Rank Correlation Measures [M]. London: Charles Griffin, 1975.

[37] WEBSTER P J, HOLLAND G J, CURRY J A, et al. Changes in tropical cyclone number, duration, and intensity in a warming environment [J]. Science, 2005, 309(5742): 1844-1846, https://doi. org / 10.1126 / science.1121564.

[38] KNAPP K R, KOSSIN J P. New global tropical cyclone data set from ISCCP B1 geostationary satellite observations [J]. J Appl Remote Sens, 2007, 1(1): 013505, https://doi.org/10.1117/1.2712816.

[39] LANDSEA C W, HARPER B A, HOARAU K, et al. Can we detect trends in extreme tropical cyclones? [J]. Science, 2006, 313(5786): 452-454, https://doi. org / 10.1126/science.1128448.

[40] KOSSIN J P, KNAPP K R, VIMONT D J, et al. A globally consistent reanalysis of hurricane variability and trends [J]. Geophys Res Lett, 2007, 34(4): 344-356, https://doi.org/10.1029/2006GL028836.

[41] HOARAU K, BERNARD J, CHALONGE L. Intense tropical cyclone activities in the northern Indian Ocean [J]. Int J Climatol, 2012, 32(13): 1935-1945, https://doi.org/10.1002/joc.2406.

[42] XIANG B Q, WANG B. Mechanisms for the advanced Asian summer monsoon onset since the mid-to-late 1990s [J]. J Climate, 2013, 26(6): 1993-2009, https://doi. org / 10.1175/JCLI-D-12-00445.1.

[43] XIAO Zhi-xiang, DUAN An-min. Can the tropical storms originated from the Bay of Bengal impact the precipitation and soil moisture over the Tibetan Plateau? [J]. Sci China Earth Sci, 2015, 58(6): 915-928, https://doi.org/10.1007/s11430-014-5028-8.

[44] LU Xiao-qin, YU Hui, LEI Xiao-tu. Statistics for size and radial wind profile of tropical cyclones in the western North Pacific [J]. Acta Meteorol Sin, 2011, 25(1): 104-112, https://doi.org/10.1007/s13351-011-0008-9.

[45] MOHAPATRA M, SHARMA M. Characteristics of surface wind structure of tropical cyclones over the north Indian Ocean [J]. J Earth Syst Sci, 2015, 124(7): 1573-1598, https://doi.org/10.1007/s12040-015-0613-6.

[46] LEI Xiao-tu, CHEN Lian-shou. A preliminary numerical study on asymmetric wind field structure of tropical cyclones [J]. Chinese J Geophys, 2005, 48(1): 31-38, https://doi.org/10.1002/cjg2.622.

[47] YUAN Jin-nan, WANG Dong-xiao, LIU Chun-xia, et al. The characteristic differences of tropical cyclones forming over the western North Pacific and the South China Sea [J]. Acta Oceanol Sin, 2007, 26(4): 29-43, https://doi.org/10.1109/UT.2007.370822.

[48] YUAN Jin-nan, WANG Dong-xiao, WAN Qi-lin, et al. A 28-year climatological analysis of size parameters for northwestern Pacific tropical cyclones [J]. Adv Atmos Sci, 2007, 24(1): 24-34, https://doi.org/ 10.1007/s00376-007-0024-y.

**Citation**: FAN Xiao-ting, LI Ying, LYU Ai-min, et al. Statistical and comparative analysis of tropical cyclone activity over the Arabian Sea and Bay of Bengal (1977–2018) [J]. J Trop Meteor, 2020, 26(4): 441-452, https://doi.org/10.46267/j.1006-8775.2020.038.